EXPERIMENTAL INVESTIGATION OF THE MICROSCOPIC DAMAGE DEVELOPMENT AT MODE I FATIGUE DELAMINATION TIPS IN CARBON/EPOXY LAMINATES

Rafiullah Khan[a], Rene Alderliesten[b], Saeed Badshah[a], M. A. Khattak[c*], M. S. Khan[c,d], Rinze Benedictus[b]

[a]Department of Mechanical Engineering, International Islamic University, Islamabad, Pakistan
[b]Faculty of Aerospace Engineering, Technical University Delft, Netherland
[c]Faculty of Mechanical Engineering, Universiti Teknologi Malaysia, 81310, UTM Johor Bahru, Johor, Malaysia
[d]School of Mechanical and Manufacturing Engineering (SMME), National University of Science and Technology (NUST), H-12, Islamabad, Pakistan

Abstract

This paper investigates the damage development ahead of mode I delamination tips in carbon /epoxy laminates using scanning electron microscope (SEM). Two techniques were adopted for the investigation; the first technique consisted of the application of stepwise load increments on DCB (double cantilever beam) specimens inside the SEM, while images were recorded until delamination onset. For the second technique, the DCB specimens were fatigue tested under different combinations of monotonic and cyclic loading. After the fatigue tests, the specimens were kept open in the microscope by insertion of steel wedges allowing the inspection of the delamination tips. The investigation revealed that multiple micro-cracks are formed parallel to the delamination growth direction ahead of the tip that coalesces. Micro-cracks that were formed 2 or 3 plies away from the delamination plane were observed to cause fibre bridging.

Keywords: Delamination, Stress ratio effect, Fractography, micro-cracks

Abstrak

Kertas ini mengkaji perkembangan kemusnahan yang lebih awal daripada mod I hujung pelekangan dalam laminat karbon/epoksi dengan menggunakan imbasan mikroskop electron (SEM). Dua teknik telah diterima pakai bagi penyiasatan itu; teknik yang pertama terdiri daripada penggunaan langkah bijak kenaikan beban terhadap specimen DCB (julur rasuk berganda) di dalam SEM, manakala imej dirakam sehingga bermulanya pelekangan. Untuk teknik kedua, spesimen DCB telah diuji untuk ujian keletihan di bawah kombinasi yang berbeza antara beban yang sama (monotonic) dan kitaran. Selepas ujian keletihan, spesimen disimpan terbuka dalam mikroskop dengan memasukkan baji keluli bagi membenarkan pemeriksaan pada hujung pelekangan. Siasatan mendedahkan bahawa pelbagai mikro-retak terbentuk selari dengan arah pertumbuhan pelekangan menjelang hujung yang bertaut. Mikro-retak yang telah terbentuk 2 atau 3 lapisan daripada satah pelekangan diperhatikan telah menyebabkan penyambungan antara gentian.

Kata kunci: Pelekangan, kesan nisbah tekanan, fraktografi, mikro-retak

1.0 INTRODUCTION

The exceptional strength and stiffness to weight ratio of composites make them a good option for weight critical structures in aerospace, automobile, marine and sports applications [1]. However, the threat of composite ply delamination is a hurdle to its wider use in primary load bearing structures. Ply delamination not only reduce the strength and stiffness of the composites but also are prone to further delamination growth and eventually failure [2].

The investigation of the delamination growth mechanism is very important for the characterization and modeling of the delamination phenomenon. The strain field ahead of a delamination/crack tip produces a process zone where complicated damage phenomena occur. Various types of damage in this zone include transverse matrix cracking and delamination among or within multiple laminae [3]. For the experimental investigation of the damage state ahead of the delamination tip, various techniques have been adopted including post mortem scanning electron microscopy (SEM) of fracture surfaces [4], in-situ SEM [5] and transmission electron microscopy (TEM) [6].The in-situ microscopy of delamination tips under mode I and mode II loading has been used by many researchers for the characterization and modeling of delamination fracture process. Because of their relevance to the current paper, a brief review of these studies is presented next.

Bradley *et al.* [5] conducted an in-situ SEM study on delamination fractures to reveal the micro-mechanism of fracture in graphite/epoxy composites under mode I, mode II and mix mode loading. The loading was applied inside SEM by pushing a blunt wedge towards the crack tip. Coats *et al.* [7] developed a residual strength prediction methodology for composite structures. Based on the experimental in-situ SEM, the developed a progressive damage methodology and used it to predict the initiation and growth of matrix cracks and fibre fracture.

Due to the microscopic phenomena at the delamination tip, Rogers *et al.* [8] adopted a different approach to study formation of micro features under mode II loading. They used shear testing of PVC foam to visually observe and describe the fracture process, developing understanding about mode II fracture in composite laminates. Tanaka *et al.* [9] investigated the stress ratio effect on mode II propagation of inter-laminar fatigue cracks in graphite/epoxy composites using in-situ SEM on the delamination tip. They observed that the delamination tip was different for positive stress ratio test compared to the negative stress ratio. For the positive stress ratios, the main crack was accompanied by small micro-cracks that were caused by principle normal stresses at an angle of 45° to the fibre direction in the plies. In case of negative stress ratios, the main crack propagated along a zigzagging path induced by principle stress reversal, causing X-shaped micro-cracks.

It is well known that when a cracked body is loaded, the crack tip experiences higher stresses due to stress concentration effect [10]. The higher stresses cause plastic deformation at the crack tip. This plastic zone depends on the loading and geometry of the specimens [11]. A similar phenomenon occurs in case of composite delamination, however due to heterogeneous nature of composite laminates, a process zone is produced at the delamination tip. The size and shape of the process zone is function of loading, type of material and delamination crack geometry [12]. Characterization of the damage type, damage density and size of the process zone can greatly enhance our understanding and modeling of the delamination growth under fatigue loading.

The objective of the current study was twofold; first, the experimental assessment of damage mechanisms ahead of mode I fatigue delamination tips, second, the relation of these mechanisms to the different features observed on the fracture surface in an earlier study using fractography. This study is in the context of a broader investigation of the effect of stress ratio on mode I fatigue delamination reported in [12-14]. The hypothesis for the current study was that for the same cyclic load range, higher stress ratios result in more damage ahead of the delamination tip. To assess the validity of the hypothesis two experimental approaches have been adopted; one with the load application in-situ SEM, and the other with the fatigue testing outside SEM and subsequent studying of the delamination tip with SEM. The details of the experiments and their results are presented in the following sections.

2.0 EXPERIMENTAL TECHNIQUES

Two experimental techniques were used to study the effect of the stress ratio on the delamination mechanism. The specimens used in both techniques were made from M30SC/DT120 prepreg. Elastic properties of the cured material are young's modulus E_1=150 GPa, transverse young's modulus E_2=7 GPa and Poisson's ratio=0.29 [15]. Fiber weight fraction of the prepreg was 66%. The procedure of the laminate manufacturing is identical as reported in [13]. The two experimental techniques are discussed in the following sections.

2.1 In-situ SEM of Damage Zone Development ahead 0f Delamination Tip in DCB Specimens under Monotonic Load Increments

The objective of the in-situ SEM examination of damage zone development was to investigate the effect of monotonic loading on the development of microscopic cracks ahead of delamination tip. It was hypothesized that for higher stress ratios, the monotonic load is higher than for lower stress ratios, resulting in more damage ahead of the delamination

tip. In this study, the edge of a DCB specimen was examined in-situ SEM during the application of quasi static load increments.

The geometry of the DCB test specimen used in this study is illustrated in Figure 1. The edges of the specimen were polished with diamond paste having sized grits equal to 0.6, 0.3 and 0.1 µm successively. After polishing, the edges were gold sputtered to avoid static charging during SEM. Aluminum blocks were bonded to the upper and lower sides of the specimens as shown in Figure 1. A hole was drilled in each block for the insertion of the pin.
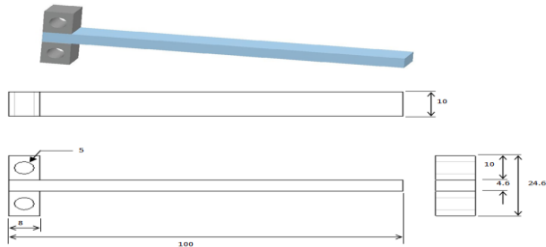

Figure 1 Geometry of DCB specimen for in-situ SEM analysis [dimensions in mm]

Four specimens (In-situ 1-4) were tested in-situ SEM under monotonic load increments at the Dutch Aerospace laboratory NLR, in Marknesse. The micro-tester mounted inside the microscope was used for the application of the load. The pins inserted into the aluminum blocks at the specimen were gripped in the micro-tester. The delamination tip on the specimen's edge was examined in SEM after each 5 N load increment. The delamination growth started at a load level equal to 35 N. The test was stopped once the delamination started.

2.2 SEM Investigation of Damage Zone Ahead of Delamination Tips in Fatigue Tested DCB Specimens

In second approach, the effect of cyclic load range and maximum load of the load cycle on the micro-crack formation ahead of the delamination tip was investigated in SEM after fatigue tests were performed at different maximum and cyclic load range conditions.

The DCB specimens were manufactured according to the same procedure as in previous section. The geometry of the specimen is shown in Figure 2. The specimen's width was equal to 10 mm. The width of current DCB was kept smaller than commonly used DCB specimen because it was tested/loaded by microtester installed inside SEM. The edges of the specimens were polished with diamond paste having sized grits equal to 0.6 and 0.1 µm successively.
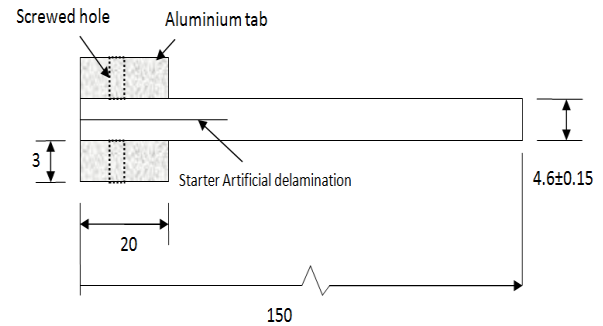

Figure 2 Geometry of the specimen for the edge SEM after fatigue tests [dimensions in mm]

In total, five specimens were fatigue tested and examined in SEM (test matrix given in Table 1). The fatigue test procedure was similar as described in [13]. The fatigue test was stopped after delamination extended up to 5 mm. After the test, the specimen was held open approximately under maximum cyclic load. A prismatic steel wedge was inserted to keep the specimen open after the test after its removal from the fatigue machine. This technique was adopted to ensure that micro-cracks are open and visible during inspection in the SEM. The edges of the DCB specimens were gold sputtered to avoid static charging during SEM.

Table 1 Test matrix for SEM investigation of damage zones ahead of delamination tip

Specimen	Delamination length [mm]	Max SERR, Gmax [J/m2]	SERR range, ΔGs [J/m2]	Stress ratio, R
SEM 01	27	81.01	20.25	0.4
SEM 02	26	79.63	19.91	0.4
SEM 03	26	79.63	19.91	0.4
SEM 04	27	81.01	20.25	0.4
SEM 05	33	84.37	54.17	0.15

2.3 Test Data Analysis

For the DCB specimens, the strain energy release rate (SERR) was calculated using the compliance technique. The relation for the SERR G is given by [16]:

$$G = \frac{P^2}{2b}\frac{dC}{da} \qquad (1)$$

Where P, a, C and b are the load, delamination length, compliance and specimen width respectively. The delamination growth rate da/dN was correlated to the SERR range ΔG_s defined as [17]:

$$\left(\Delta\sqrt{G_s}\right)^2 = \left(\sqrt{G_{max}} - \sqrt{G_{min}}\right)^2 \qquad (2)$$

Where G_{max} and G_{min} are maximum and minimum SERR respectively.

3.0 RESULTS

3.1 In-situ SEM Examination of the DCB Specimen Edges During Monotonic Loading

As mentioned in section 2, the specimens were loaded by the micro-tester inside the microscope. During the test, the delamination tip was continuously monitored. It was difficult to capture high-quality images during the load application, because of high magnification microscopy and moment of the target location (delamination tip) due to deformation of the specimen. For this reason the loading was stopped after every load increment of 5 N, and a SEM image of the tip was then taken. The delamination started to grow at a load equal to 35 N. Seven SEM images were taken during loading. There was no obvious difference between the images taken before the delamination onset. Figure 3 shows a typical SEM image of the delamination tip at 35 N, just before delamination onset. Delamination growth direction is from left to right of the image. The matrix layer in the delamination plane can be seen as stretched at the right side of the image as compared to the left side as shown by red arrows in the image. No micro-cracking (cracks in the matrix layer between adjacent plies) was observed during loading up to 35 N.

The delamination growth was sudden as the load level crossed 35 N. Since the magnification of the SEM was high, the delamination tip was out of focus at that moment. The loading was stopped and it was observed that delamination had extended about 1 mm.
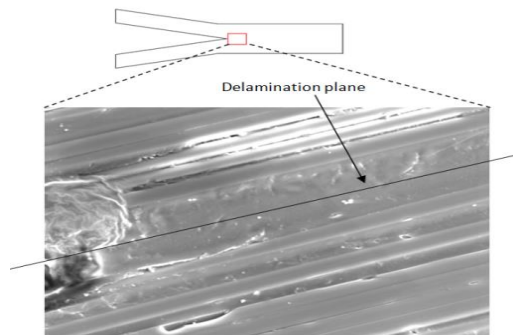

Figure 3 SEM image of the tip of the DCB specimen at 35 N, magnification X300 (Delamination growth direction from left to right)

The SEM image of the delamination tip after the extension of 1 mm is shown in Figure 4. The figure shows two damage types in the vicinity of the delamination tip. These damage types are micro-cracks in the matrix layer and debonding of the fibres and matrix. It was observed in all cases that micro-cracks crossed the matrix layer touching both upper and lower fibres of the adjacent layers. The size (length) of the micro-cracks is not same. Figure 4 shows fully grown micro-cracks just before delamination growth where the intact matrix can beseen as ligament bridging the delamination plane plies. The formation of hackles is

often attributed to the coalescence of micro-cracks [12, 18]. In that case it would be expected that delamination locally jumps from one plane to another. The damage mechanisms are not confined only to the delamination plane.
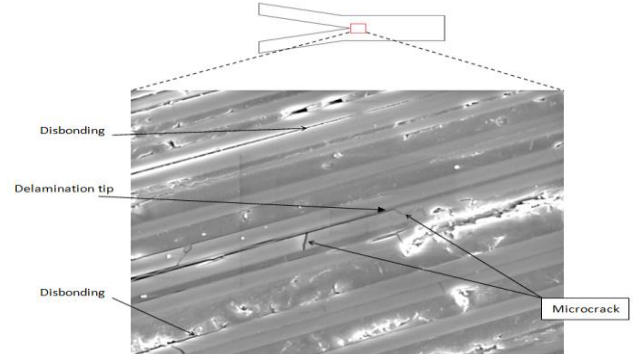

Figure 4 Matrix ligament bridging at the delamination tip (X300), In-situ 1, (Delamination growth direction from left to right)

Debonding between plies in a range of 2-3 plies was observed in the upper and lower plies of the delamination plane as shown in Figure 5.
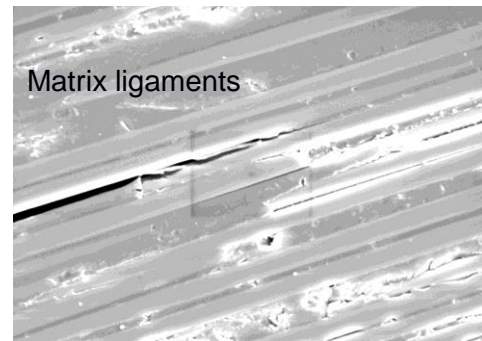

Figure 5 SEM image of the tip of the DCB specimen after delamination growth, In-situ 1, magnification X300 (Delamination growth direction from left to right)

3.2 SEM Examination of the Edges of the DCB Specimens after Fatigue Tests

This section presents the results of the SEM investigations on the edges of the DCB specimens that were tested under fatigue. Figure 6 shows a typical SEM image of the delamination tip of a specimen. The existence of cracks/disbanding ahead of the delamination tip can be seen in the image. The size of these cracks decreases as the distance from the tip is increased. These cracks are not in one plane (i.e. in-line with main delamination), instead they are alternatively changing position above and below the delamination plane. The coalescence of these cracks/disbanding results in the delamination extension. However, in that case the delamination locally jumps in its path around the global delamination plane.
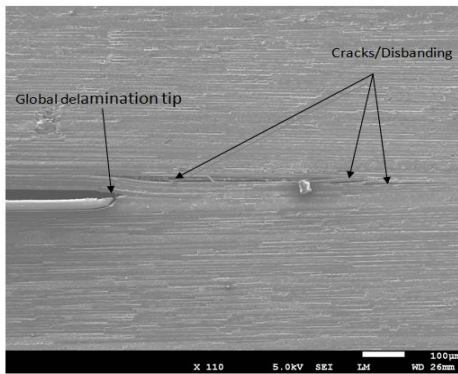
Figure 6 SEM image of the delamination tip, Specimen SEM 3 (G_{max}=79.6 J/m²), magnification X110 (Delamination growth direction from left to right)

The local shift in the delamination plane involves several fibres above and below the plane that later on results in bridging fibres as shown in the figure. A clearer SEM image showing bridging fibres in the delamination wake behind the tip is shown in Figure 7.
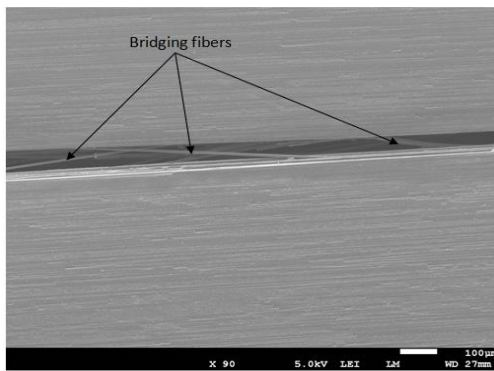

Figure 7 Bridging fibres in delamination wake, SEM 3, X90 (Delamination growth direction from left to right)

Figure 8a shows micro-cracks in the matrix layer between adjacent plies in the specimen In situ 4. Three delamination fronts/ disbanding can be seen in the figure, acknowledging alternation of local delamination plane as discussed in the previous paragraph. Figure 8b is the magnified view showing details of the micro-cracks ahead of delamination tip. It can be seen that the micro-cracks are approximately parallel to the fibres of the adjacent plies and also parallel to the delamination growth direction, however some micro-cracks are slightly oriented to the adjacent ply.
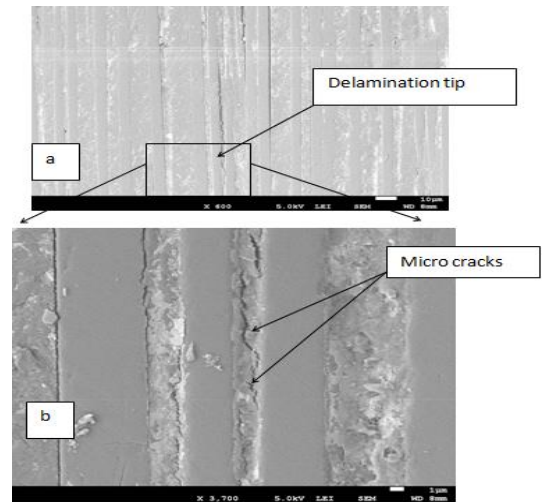

Figure 8 SEM images of the delamination tip, Specimen SEM 4 (G_{max}=81 J/m²), (a) magnification X600 (b) magnification X2300, (Delamination growth direction from top to bottom)

The density/number of micro-cracks may depend on many factors like the number of fatigue cycles, the level of loading and the local thickness of matrix between adjacent fibres. Figure 9 illustrates SEM image of the delamination tip in the specimen SEM 5. The density of the micro-cracks in this figure is much higher as compared to Figure 8.
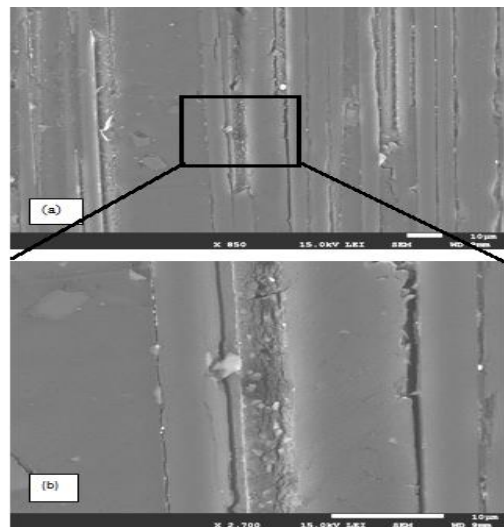

Figure 9 SEM images of the delamination tip, Specimen SEM 5 (G_{max}=84.4 J/m²),, (a) magnification X850 (b) magnification X2700 (Delamination growth direction from top to bottom)

4.0 DISCUSSION

4.1 In-situ Edge Observations on DCB Specimen

The current experimental study revealed the formation of microscopic fractures near the delamination plane ahead of the delamination tip. This observation confirms observations reported

before in the literature [5], i.e. formation of micro-cracks and their relation to the loading.

Despite these observations, the authors believe that these in-situ tests are not entirely straightforward. As discussed in earlier work of the current authors [12], the delamination plane consists of debonding of fibres from the matrix, resulting in the observations of striations in the fibre imprint in the matrix, and of micro-cracking of the matrix. Microscopically, the first fracture mode is considered adhesive failure, while the second mode is considered cohesive failure.

The challenge with observing the fracture from the specimen's edges is that the observation is entirely dependent on the exact microscopic configuration of the delamination plane at the specimen's edge. It may be argued that due to crack tunnuleing, the delamination front adopts thumb-like shape due to plain strain condition in DCB specimens; nevertheless the delamination growth rate under fatigue is uniform throughout specimen's width.As reported before[12], the delamination plane observed with microscopy approximately consists for about 80% of fibre/matrix debonding and for about 20% of matrix cracking. In unidirectional laminates, the fibres are parallel to the specimen's edge, which implies that the edge can be assumed to be true representative of the process further from the edge.

To validate the reproducibility of the observations reported here, 4 similar cases were tested for mode I fatigue loading. All cases had a stress ratio of R=0.4, with similar delamination lengths, and similar maximum SERR and SERR range values. It is concluded that the observations are fairly consistent over these four tested cases.

4.2 Observed Features at Delamination Tip

Post-mortem investigation of fatigue delamination fracture surfaces, reported in earlier work, revealed the presence of multiple features like hackles, striations in the fibre imprint, broken or pulled-out fibres.

In the current study, it is observed that the macroscopic delamination tip is preceded by micro-crack formation in the matrix approximately in the plane of the delamination. At the microscopic level, these micro-cracks were observed to be not exactly positioned at the plane ahead of the lead-delamination tip, but at varying distances from that plane. In all observed cases however, the cracks propagated parallel to the direction of the lead-delamination. Depending on the misalignment of these micro-cracks, the formation of two different features was observed. In most cases, microscopically small misalignments led to the formation of hackles in the matrix at the moment these micro-cracks coalesce. Occasionally, the misalignment covered a distance including some fibres bundles, leading to the formation of bridging fibres, as illustrated by the Figures 6 and 7.

The formation of hackles is consistent with earlier reported observations of delamination fracture surfaces created under mode I loading. Where for example mode II loading results in micro-cracks under an angle with the main delamination plane, yielding shear cusps under coalescence of these micro-cracks [9], the coalescence of the parallel micro-cracks in mode I results in hackles[13].

The formation of the hackles is primarily attributed to the misalignment of the micro-cracks, i.e. it is not specifically caused by either quasi-static or fatigue loading. This can be substantiated by the fact that these features were both observed in the quasi-static in-situ delamination tests, as well as in the fatigue delamination tests [19, 20].

What is deemed of interest here is that there seems to be more than just a single delamination plane when observed at a microscopic level. For example, Figure 4 illustrates that multiple parallel cracks are being formed of which the lead delamination in its plane remains the dominant one. This implies that studies reporting the delamination fracture surfaces using microscopy do not reveal the fact that subsurface other delamination fractures may be present. In particular studies that attempt to relate the strain energy dissipation to the formation of fractures [21, 22], should consider that the fracture features observed with microscopy fail to reveal these subsurface fractures.

4.3 Influence of Load Cycle Range

The present experiments were performed in the context of a broader study addressing the stress ratio effect generally observed in mode I fatigue delamination studies. The idea here was to identify whether the microscopic damage state in the delamination tip vicinity and ahead of the delamination tip would be affected by the stress ratio.

The current experiments allow to discuss the influence of the load range on the formation of micro-cracks, by comparing the cases R=0.15 and R=0.4. The maximum SERR G_{max} for the tested cases was approximately the same. The main difference between the two stress ratios was the SERR range ΔG_s.What was observed is that the amount of micro-cracks formed ahead of the delamination tip is different. The higher SERR range, equivalent to a lower stress ratio, revealed more micro-cracks formed. This is illustrated with comparing the Figures 8 and 9. However, the authors believe that firm conclusions cannot be drawn from the present observations alone, because aside from the maximum level and range of SERR, it is believed that the amount of cycles may influence the formation and propagation of these micro-cracks as well. Hence, to be able to attribute the amount of micro-cracks formed to the load components, more data is required.

Nonetheless, the authors do believe that the current approach of in-situ delamination growth monitoring yields information that can shed more light on the topic of the stress ratio effect in mode I delamination. The fact that tests can be performed that specifically keep the maximum SERR or the SERR range constant, while the micro-crack formation is

monitored in-situ, may allow for development of a more quantitative relationship between stress ratio and delamination growth.

4.4 Influence of the Maximum Load in the Cycle

The influence of the stress ratio on delamination growth may also be viewed from the perspective of maximum load in the load cycle. If for example the SERR range ΔG_s is kept constant, a higher stress ratio implies the application of a load cycle with a higher maximum load. Hence, the contribution of the maximum load to the formation of micro-cracks ahead of the delamination should be quantified. For this reason, the quasi-static tests were performed where at increments of 5 N the delamination tip was monitored.

As expected, the maximum load has a significant influence on the delamination growth. Once the load of 35 N was exceeded the delamination onset was observed. The further the load is increased the more delamination growth and formation of micro-cracks occurred. Thus higher stress ratios are equivalent to load cycles with a relatively high minimum load and a higher maximum load compared to low stress ratios. This means that the extension and formation of micro-cracks will greater for high maximum SERRs.

With the influence of the SERR range, discussed in the previous section, in mind, no conclusive relationship can be developed. It is believed that more data is required generated with in-situ delamination tests to allow for a more quantitative correlation.

5.0 CONCLUSIONS

This paper presents the experimental study on the formation and propagation of delamination in fibre reinforced polymer composites. Both quasi-static and fatigue delamination tests on DCB specimen were monitored in SEM to reveal the formation of microscopic damage ahead of the macroscopically observed delamination tip.

It is concluded that observations with the in-situ SEM delamination tests are dependent on the configuration of the interface at the specimen's edge. Hence, the observation that can explain both the striation formation in the fibre imprint of the matrix and the hackle formation is impossible. Only the formation of hackles can be illustrated with these tests. The observation for this feature is consistent as demonstrated with the duplication of tests at R=0.4. The results revealed the relation between fracture mechanisms and fatigue loading. Both load components, i.e. the maximum SERR and the SERR range, influence the formation of micro-cracks ahead of the delamination tip.

References

[1]   Khan, R. 2013. Delamination Growth in Composites under fatigue. PhD Thesis. TU Delft Netherland.
[2]   Harris, B. 2003. *Fatigue in Composites*. Science and Technology of the Fatigue Response of Fiber Reinforced Plastics. Cambridge: Woodhead Publishing Ltd.
[3]   Ritchie, R. O. 1988. Mechanisms of Fatigue Crack Propagation in Metals, Ceramics and Composites: Role of Crack Tip Shielding. *Materials Science and Engineering A*. 103(1): 15-28.
[4]   Greenhalgh and Emile. 2009. *Failure Analysis and Fractography of Polymer Composites*. Elsevier: Woodhead Publishing Limited.
[5]   Bradley, W. L. and Cohen, R. N. 1985. Matrix Deformation and Fracture in Graphite-Reinforced Epoxies. In Delamination and Debonding of Materials. *ASTM International STP*. 876: 389-410.
[6]   Sue, H. J., Jones, R. E., and Garcia Meitin, E. I. 1993. Fracture Behavior of Model Toughened Composites under Mode I and Mode II Delamination. *Journal of Materials Science*. 28(23): 6381-6391.
[7]   Coats, T. W., and Harris, C. E. 1999. A Progressive Damage Methodology for Residual Strength Predictions of Notched Composite Panels. *Journal of Composite Materials*. 33(23): 2193-2224.
[8]   Rogers, C. E., Greenhalgh, E. S., and Robinson, P. 2008. Developing a Mode II Fracture Model for Composite Laminates. *ECCM13*.
[9]   Tanaka, K., and Tanaka, H. 1997. Stress-ratio Effect on Mode II Propagation of Inter-laminar Fatigue Cracks in Graphite/epoxy Composites. Composite Materials: Fatigue and Fracture. *ASTM*. 1285: 16.
[10] Inglis, G. R. 1957. Analysis of Stresses and Strains near the End of a Crack Traversing a Plate. *Journal of Applied Mechanics*. 24: 361-364.
[11] Irwin, G. R. 1985. *Fracture Handbuch der physik VI*. S. Flugge New York: Springer-Verlag.
[12] Khan, R., Alderliesten, R. and Benedictus, R. 2014. Two-Parameter Model For Delamination Growth Under Mode I Fatigue Loading (Part B: Model Development). *Composites Part A: Applied Science and Manufacturing*. 65: 201-210.
[13] Khan, R., Alderliesten, R. and Benedictus, R. 2014. Two-Parameter Model for Delamination Growth under Mode I Fatigue Loading (Part A: Experimental study). *Composites Part A: Applied Science and Manufacturing*. 65: 192-200.
[14] Khan, R., Alderliesten, R., Yao, L. and Benedictus, R. 2014. Crack closure and Fibre Bridging during Delamination Growth in Carbon Fibre/Epoxy Laminates under Mode I Fatigue Loading. *Composites Part A: Applied Science and Manufacturing*. 67: 201-211.
[15] Rodi, R.2012. The Residual Strength Failure Sequence In Fiber Metal Laminates. PhD Thesis, Aerospace Faculty Tu Delft Nederland.
[16] ASTM. 2007. Standard Test Method for Mode I Interlaminar Fracture Toughness Of Unidirectional Fiber-Reinforced Polymer Matrix Composites. D5528-01
[17] Rans, C. D., Alderliesten R. and Benedictus R. 2011. Misinterpreting The Results: How Similitude Can Improve Our Understanding Of Fatigue Delamination Growth. *Composite Science and Technology*. 71: 230-238.

[18] Lee, S. M. 1997. Mode II Delamination Failure Mechanisms of Polymer Matrix Composites. *Journal of Material Science.* 32: 1287-1295.
[19] Bascom, W. D., Boll, D. J., Hunstun, D. L., Fuller, B. and Phillips P. J. 1987. Fractographic Analysis of Interlaminar Fracture. Toughned Composites. *ASTM STP.* 937: 131-149.
[20] Hojo, M., Tanaka,K., Gustafson, C-G. and Hayashi R. 1987. Effect of Stress Ratio on Near-Threshold Propagation of Delamination Fatigue Cracks in Unidirectional CFRP. *Composites Science and Technology*. 29(4): 273-292.

[21] Pascoe, J. A., Alderliesten, R. C. and Benedictus, R. 2015. On the Relationship between Disbond Growth and the Release of Strain Energy. *Engineering Fracture Mechanics.* 133: 1-13.
[22] Yao, L., Alderliesten, R., Zhao, M. and Benedictus, R. 2014. Discussion on the Use of the Strain Energy Release Rate for Fatigue Delamination Characterization. *Composites: Part A.* 66: 65-72.